Energy 309 (2024) 133110

Contents lists available at ScienceDirect

Energy

journal homepage: www.elsevier.com/locate/energy

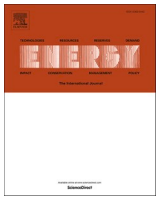

Design, construction and operation of a special electric vessel for water-city utilities service

Massimo Guarnieri [a,b,*], Angelo Bovo [c], Nicolò Zatta [a,b], Andrea Trovò [a,b]

[a] Department of Industrial Engineering, University of Padua, via Gradenigo 6a, 35131, Padova, Italy
[b] Interdepartmental Centre Giorgio Levi Cases for Energy Economics and Technology, University of Padua, via Gradenigo 6a, 35131, Padova, Italy
[c] Veritas SpA, via Porto di Cavergnago 99, 30173, Venice, Italy

ARTICLE INFO

Handling editor: X Ou

Keyboards:
Electric vessel
Hybrid powertrain
Waterborne mobility
Battery electric vessel
Venice

ABSTRACT

This article presents an electric vessel for technical service that has been designed, constructed and put into service in Venice, Italy. It is a prototype in a program for replacing an existing fleet of 63-kW diesel boats. It had to preserve the present 12-m boats size, maneuverability with a 360° steering azimuth propeller, and onboard power drives, namely a large waste caisson with a compacting drawer, a crane for moving bins, and a collapsible cockpit for passing low bridges. The design was developed on the power and work demand acquired in a preliminary measurement campaign. Onboard drives had to provide full service at zero emission in most routes inside the historical city. Two 50-kW permanent magnet electric motors were chosen to power the propeller and the compactor, and smaller motors for other drives. The series hybrid powertrain has an 80-kWh lithium-iron-phosphate battery, flanked by a small 15-kW biodiesel generator as a range extender. The boat demonstrated to ensure a fuel saving of 72%–100% and an operating energy cost saving of 20%–36%, depending on the route driven in hybrid or full electric mode. The prototype is expected to contribute to a wider transition to waterborne electric mobility in Venice.

Nomenclature

Symbols	
A_c	constant in Li-ion cell model [V]
B_c	constant in Li-ion cell model [−]
C_{bd}	biodiesel cost [€]
C_{el}	electricity cost [€]
C_{ice}	ICE boat routing cost [€]
C_{tot}	PHEB1 routing cost [€]
E_d	battery energy density [Wh kg^{-1}]
E_{lib}	battery energy [kWh]
E_s	battery specific energy [Wh L^{-1}]
i	cell current [A]
i^*	low pass filtered cell current [A]
K_r	coefficient in Li-ion cell model [Ω]
K_v	coefficient in Li-ion cell model [Ω s^{-1}]
LC	rated life cycle [−]
N_{cell}	number of cells in series per module [−]
NCV_{bd}	biodiesel net calorific value [kWh kg^{-1}]
N_m	number of modules in series [−]
N_p	number of cells in parallel per module [−]
p_{bd}	biodiesel price [€ L^{-1}]
P_{bdg}	BDG power [kW]

(*continued on next column*)

(*continued*)

$P_{bdg\text{-}ls}$	BDG power losses [kW]
P_d	battery power density [W kg^{-1}]
P_{dr}	total drive power [kW]
p_{el}	electricity price [€ kWh^{-1}]
P_i'	power of the i-th hydraulic circuit [kW]
$P_{lib\text{-}ls}$	battery power losses [kW]
P_{lib}	battery power [kW]
$P_{lib,rated}$	battery rated steady state power [kW]
$P_{lib,peak}$	battery peak power [kW]
P_s	battery specific power [W L^{-1}]
Q_i	oil flow rate in the i-th hydraulic circuit [L min^{-1}]
Q_{lib}	battery capacity [Ah]
R_i	cell internal resistance [mΩ]
R_{ic}	constant resistance term in Li-ion cell model [Ω]
S_{bd}	relative fuel saving [%]
S_{cost}	relative energy cost saving [%]
S_s	BDG switch state [−]
T	route duration [h]
T_{op}	rated operating temperature [°C]
V_{bd}	BDG consumed biodiesel volume [L]
V_{co}	constant term in Li-ion cell model [V]
V_{ice}	ICE consumed biodiesel volume [L]

(*continued on next page*)

* Corresponding author. Department of Industrial Engineering, University of Padua, via Gradenigo 6a, 35131, Padova, Italy
E-mail address: massimo.guarnieri@unipd.it (M. Guarnieri).

https://doi.org/10.1016/j.energy.2024.133110
Received 21 March 2024; Received in revised form 4 September 2024; Accepted 5 September 2024
Available online 5 September 2024

(*continued*)

V_{lib}	battery voltage [V]
W_{bdg}	BDG delivered work [kWh]
W_{del}	battery delivered work [kWh]
W_{dr}	total drive work [kWh]
W_{el}	grid provided electric work [kWh]
W_i'	work of the *i*-th hydraulic circuit [kWh]
W_{lib}	battery delivered work [kWh]
w_m	module weight [kg]
Δp_i	pressure drop in the i-th hydraulic circuit [bar]
η_{bdg}	biodiesel generator efficiency [−]
ρ_{bd}	biodiesel density [kg L^{-1}]
τ	sampling step [s]
Acronyms	
AC	Alternating current
B	Propulsion backward
BDG	Biodiesel generator
BMS	Battery management system
CAGR	Compound annual growth rate
CAPEX	Capital expenditure
CDCS	Charge-depleting charge-sustaining
CODLAG	Combined diesel-electric and gas
CODLOG	Combined diesel-electric or gas
Comp	Compactor
CrCoS	Crane cockpit and services
DC	Direct current
DOD	Depth of discharge
ECMS	Equivalent fuel consumption minimization strategy
EM	Electric motor
EMS	Energy management system
F	Propulsion forward
FE	Full electric
HMI	Human Machine Interface
ICE	Internal combustion engine
IEP	Integrated electric propulsion
IGBT	Insulated-gate bipolar transistor
LCA	Life cycle assessment
LCOE	Levelized cost of energy
LIB	Lithium-ion battery
PHEB1	Plug-in hybrid electric boat one
PID	Proportional integral derivative
PMS	Power management system
PMSM	Permanent magnet synchronous motor
SOC	State of charge
SOH	State of health
VFD	Variable-frequency driver

1. Introduction – electric watercraft overview

The *turbo-electric transmission* and *diesel-electric transmission* in water vessels, which consist of thermal engines coupled with electric generators feeding the electric motors (EMs) that power the propellers, were successful developed through the 20th century due to speed decoupling between thermal prime movers and propellers. More complex *integrated electric propulsion* (IEP) schemes, which are normal practice in large ships, are the *combined diesel-electric and gas* (CODLAG), in which the propeller shafts are moved by EMs powered by diesel generators and gas turbines intervene at higher speeds, and the *combined diesel-electric or gas* (CODLOG), in which only a type of drive works at a time. Altogether, these propulsion schemes constituted forms of *hybrid electric* powertrains either *series* (if the propellers are only driven electrically) or *parallel* (in the opposite case) which only in recent years may have incorporated batteries providing electric energy storage. They exploit simple gearboxes, versatile varying-speed electric propulsion and possible use of high-maneuverable azimuthal thrusters. Small boats with *full electric* (FE) powertrains, and no thermal engine, have been put on the market for short-range niche uses by a dozen of companies since the 1970s, in some cases reaching mass production. FE vessels have attracted increasing interest in last few decades, on the push of a new regulation to cut down emissions issued by agencies such as the International Maritime Organization [1] and several small prototypes have been built. *Alsterwasser*, the first FE passenger vessel powered by fuel cells, was put into service in the Alster lake in Hamburg, Germany, in 2008 [2]. It uses two 48-kW PEM fuel cells fed from 50-kg hydrogen tanks and a lead-acid battery to provide zero-emission and silent navigation. Before this, fuel cell maritime navigation was only used in navy submarines [3]. The 31-m German-Swiss yacht *MS Tûranor PlanetSolar*, propelled by two 60-kW EMs fed by a 93-kW photovoltaic (PV) generator and Li-ion battery, circumnavigated the globe between 2010 and 2012 [4]. At a larger level, Norwegian shipyard Fjellstrand built *FM Ampere*, an 80-m ferry propelled by two 450-kW EMs powered by a 1460-kWh Li-ion battery that exploits fast-recharging facilities at each docking. It entered service in a Norwegian fjord in February 2015 [5].

Market forecasts estimate that the global market of electric ships will grow at a compound annual growth rate (CAGR) of ca. 14% in the period 2022–2030, exceeding $ 16 billion by 2031 [6,7]. In this framework, large full and hybrid electric ships, both commercial and naval, have attracted a substantial body of research and development (R&D) and many papers have been presented and published. Some remarkable papers reviewing the subject are presented in [8–13]. Small to medium electric vessels have raised less attention in the scientific literature, despite they are an attractive option in short-medium-range internal waters, harbor cities (e.g., Venice, Amsterdam, Hamburg, and Stockholm) and in historical and environmentally sensitive lakes, fjords, coastal lagoons, and archipelagos (e.g., Kornati, Cyclades, and Skärgårdshavet) [14–16].

This paper presents the design, construction and field-testing of a prototype plug-in hybrid electric boat for navigation in the internal waters of Venice, Italy, that is provided with battery storage diesel-generator range extender and features an unusually complex electric system needed to service as waste collector. The boat has been designed, built, field-tested and put into regular service by the city utility Veritas SpA with the scientific support of the University of Padua.

2. Water mobility and waste collection in venice

The city of Venice, in the eponymous lagoon in North-East Italy, has no street and mobility takes place in its canals and water alleys (Fig. 1). Water buses and water taxis provide public transportation, while private transportation uses boats not much different from the latter. Freights are moved with vessels long up to 20 m and larger barges. Special vessels provide dedicated services. These varied fleets are almost completely powered with diesel engines, often old and heavily polluting [17]. Diesel noise and vibrations disturb residents and the tourists visiting the city all over the year. Only a handful of prototype vessels have electric powertrains, and mostly not of a cutting-edge technology. Within the general roadmap of a climate-neutral European Union by 2050, the Venice Municipality has undertaken programs for decarbonizing energy and mobility in the city and its lagoon. In such framework, the public multi-utility Veritas SpA was appointed to develop a wide project funded by the Italian Ministry for Environment and Land and Sea Protection [18] that includes the shipbuilding of electric utility-service boats, constituting prototypes for the future electrification of its whole fleet. One of these prototypes is the boat reported in this paper, that consists of a hybrid diesel-battery waste-collecting vessel featuring six power drives for motorized operations. It was conceived to potentially replace the internal combustion engine (ICE) boats presently used in everyday waste-collection, to navigate at zero emissions and minimal noise in the service routes inside the historical city and to use a low-emission thermal engine along a few longer routes outside the historical city.

Veritas SpA provides some waterborne services to the city of Venice and the surrounding islands in the lagoon, including waste collection and processing and maintenance of the drinking water network. The present Veritas waste-collection fleet consists of over 80 technical boats, 70 of which are operated daily along several routes long up to 6 km. To reach all collection points, these routes extend along narrow canals and twisting water alleys crossed by low pedestrian bridged, where

Fig. 1. Satellite view of the intricated topography of Venice, with 3 named neighborhoods out of 6 (Cannaregio, Castello, Giudecca), Murano Island and surrounding minor Islands (courtesy of ESA).

navigation may be challenging. Garbage bins filled with sorted waste are hand-moved to the collection points aside water alleys, where the waste-collecting vessels dock, lift the bins with a crane and empty them into an on-board caisson (Fig. 2). Waste is therein compressed by a double-room compactor to maximize loading capacity. After completing their routes, the vessels return to the dock, where an industrial crawler crane picks up the caissons and empties them onto 470/1050 tons barges, which are then towed to the mainland waste site, where garbage is processed almost entirely. About 600 m^3 of waste are collected and processed daily.

The present standard Veritas waste-collecting vessel has a hull of 12 m × 2.7 m × 1.3 m displacing 18.5 ton. A single pilot operates each vessel and most have a closed cockpit hosting him. The vessels are provided with five power drives controlled by the pilot.

- azimuthal propeller,
- 360° azimuthal steering and hoister (for shallow water navigation and real time propeller maintenance),
- caisson waste compactor,
- five-movement crane,
- collapsing cockpit (for low bridges passing).

The standard vessel is powered by a 95-kW diesel ICE that drives three pumps pressurizing four mineral-oil hydraulic circuits which in turn power the five drives above.

A. propulsion (propeller + steering) forward (F),
B. propulsion (propeller + steering) backward (B),
C. caisson waste compactor (Comp),
D. crane and services (cockpit and others minor services, CrCoS).

Despite their versatility and operability, these diesel ICE vessels are burdened by mechanical cumbersome powertrains, from the gearboxes moving the pumps down to the hydraulic drives.

3. Preliminary measurement campaign

Power and work rating for the prototype vessel were determined on

Fig. 2. A Veritas waste-collecting vessel lifting a land bin with the crane and emptying it into the caisson.

consumption data in real service, obtained after a measurement campaign carried out on a specifically instrumented ICE vessel in standard service during a period of two months along the routes Castello, Cannaregio and Giudecca, which are inside the historical city, and the routes Islands and Murano, which reach some surrounding minor islands and a larger one at short distance from the city, respectively, all inside the lagoon (Fig. 1). Each *i*-th hydraulic circuit above was equipped with transducers measuring oil flow rates Q_i [L min^{-1}] and pressure drops Δp_i [bar], which were acquired at sampling steps $\tau_j = 1$ s during the measurement campaign. From these measured data, the power profile $P_i'(\tau_j)$ and consumed work W_i' along the routes were computed:

$$P_i'(\tau_j) = Q_i(\tau_j)\ \Delta p_i(\tau_j) \,/\, 600\ [\text{kW}] \tag{1}$$

$$W_i' = (\tau_j \,/\, 3600) \sum_j P_i'(\tau_j)\ [\text{kWh}] \tag{2}$$

The net power P_i and work W_i demands in the four hydraulic circuits were obtained amending the results of eq. (1) and eq. (2) from the boost pump consumption (which only works to maintain the pressure in the four hydraulic circuits). For the sake of example, Fig. 3 presents the circuit power profiles along the Giudecca route, showing many spiky peaks and a low average value. Table 1 summarizes the peak power and consumed work in the four hydraulic circuits: forward and backward propulsion (Prop. F&B), compactor (Comp), and crane, cockpit and services (CrCoS) along the five test routes. The boat peak power values P_{dr} result from the simultaneous power demands of the four hydraulic circuits whereas the boat route work values W_{dr} are the sum of the work demands of the four hydraulic circuits along the whole route. $P_{ave} = W_{dr}/T$ is the route average power (ranging as 9.7–20.7 kW), $E_{ice} = V_{ice}\ \rho_{bd}\ NCV_{bd}$ is the energy supplied to the ICE (where $\rho_{bd} = 0.88$ kg L^{-1} is the biodiesel density and $NCV_{bd} = 10.35$ kWh kg^{-1} is its net calorific value) and $\eta = W_{dr}/E_{ice}$ is the energy efficiency along the whole route (ranging as 15.5%–25.0%). The ICE power rating of 95 kW ensures supplying all peak power P_{dr} but the average power P_{ave} is much lower in all routes, as shown in Fig. 3 and highlighted by the ratios P_{ave}/P_{dr} (ranging as 16.6%–32.7%), so that the ICE operates far from its optimal working point, which implies the low efficiency η shown in Table 1.

4. Plug-in hybrid electric boat 1 – PHEB1

4.1. Literature investigation

A preliminary analysis of the literature provided an insight of the state-of-the-art technologies of electric vessels, although most papers refer to ships larger than the vessels here considered. A strategic approach to the design of ships, with stages and methodologies, was presented by Chalfant [19], while the exploration of the design space for large ships by means of analytical methodology (TIES) was proposed by Mcnabb et al. [20] with the aim of identifying the tradeoffs of technologies and the design that optimizes sets of figures of merit. McCoy provided knee comparisons of hybrid electric propulsion schemes for ships [21,22] while hybrid, integrated and all-electric power systems for ships were studied by several other authors, including Zahedi et al. [23], S.Y. Kim et al. [24], Sulligoi et al. [25], and Thongam et al. [26]. The importance of standards in electric ship design was discussed by Y. Khersonsky [27].

The battery energy storage was investigated by K. Kim et al. [28] and by Malla et al. [29], among others. K. Kim et al. also proposed a numerical analysis of battery-generator hybrid electric powertrains for ships and compared them with conventional generators-only solutions [30]. The modelling and simulation of electric system in vessels with all-electric hybrid power system was proposed by several authors, notably by Zahedi et al. [31], while Kanellos et al. investigated the optimal design of power generation and demand adjustment in all-electric ships by means of dynamic programming techniques [32], with a particular attention to onboard energy storage system [33]. A predictive control algorithm to manage the electric work flow and storage device was studied by Vu et al. [34]. An acute analysis on power flow control system stability in all-electric ships was proposed by M. Cupelli et al. [35] while Hebner presented keen insight on the replacement of the hydraulic system with electric actuators [36]. A review of the designs and controls of hybrid powertrains in electric ships was developed by Geertsma et al. [37], recognizing that advanced controls in hybrid architectures can provide a reduction of fuel consumption and emissions up to 10%–35%. J. Barros et al. [38] provided an extensive review of the main contributions to power quality in ships in the light of present regulations for electrical installations in ships. An efficiency analysis was presented by Nuchturee [39], considering intelligent power

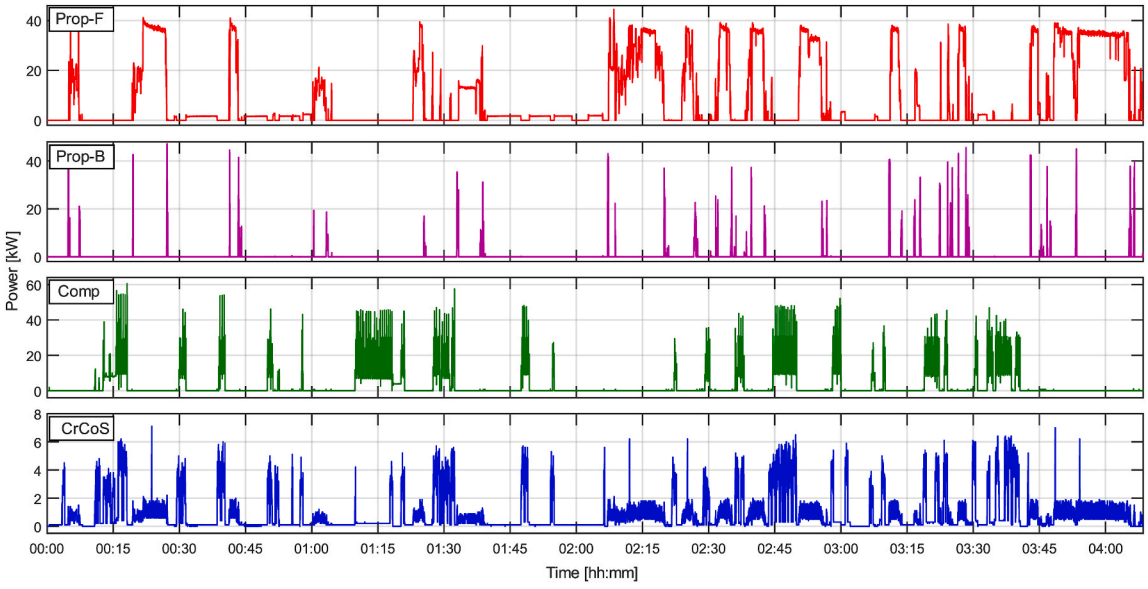

Fig. 3. Power demands in the four hydraulic circuits of the ICE vessel during a 4-h service in the Giudecca route. Prop = propulsion (F = forward, B = backward), Comp = compactor, CrCoS = crane cockpit and services. The profiles present many spikes and a low average value, for which a battery-powered electric propulsion is naturally suited.

Table 1
Measurement campaign on an ICE vessel: peak power and work of the four hydraulic circuits (HCs) in five test waste-collection routes. T = duration, V_{ice} = ICE consumed fuel, Prop = propulsion (F = forward, B = backward), Comp = compactor, CrCoS = crane, cockpit and services.[1] The total drive peak power P_{dr} results from the simultaneous power demands from the four HCs (Pro F&B, Comp and CRCoS).[2] The total drive work W_{dr} is the sum of the work demands from all HCs along the whole route. $P_{ave} = W_{dr}/T$ is the route average power; $E_{ice} = V_{ice}\,\rho_{bd}\,NCV_{bd}$ is the energy supplied to the ICE (where $\rho_{bd} = 0.88$ kg L^{-1} is the biodiesel density and $NCV_{bd} = 10.35$ kWh kg^{-1} is its net calorific value); $\eta = W_{dr}/E_{ice}$ is the energy efficiency along the whole route.

Routes	T [h]	V_{ice} [L]	HC peak power P_i [kW]				HC route work W_i [kWh]				P_{ave} [kW]	E_{ice} [kWh]	η [%]
			Prop F&B	Comp	CrCoS	Tot Drive[1]	Prop F&B	Comp	CrCoS	Tot Drive[2]			
Cannaregio	4.67	32.1	50.2	50.5	5.5	56.0	34.0	9.6	1.8	45.4	9.7	292.5	15.5
Giudecca	4.13	28.4	53.4	60.4	7.1	67.5	36.8	6.8	2.6	46.2	11.2	259.1	17.8
Castello	4.48	40.8	52.8	49.3	6.4	55.7	57.2	5.6	1.9	64.7	14.4	372.1	17.4
Murano	4.57	41.6	51.0	56.6	6.8	63.4	82.8	9.2	2.6	94.6	20.7	379.0	25.0
Islands	5.33	48.6	45.7	57.7	6.6	64.3	92.8	7.4	2.9	103.1	19.3	442.6	23.3

management in powertrains integrated with energy storage. A simulation of a powertrain powered by a hybrid electric system made of fuel cells and batteries for a ferry in Denmark targeting optimal operation in terms of hydrogen consumption and fuel-cell degradation is presented in [40]. Series, parallel and series-parallel hybrid power systems have been analyzed and compared by Yuan in [41]. A life cycle cost assessment (LCCA) of different powertrain architectures was published by Perčić [42]. An interesting method for the suppression of thrust loss due to cavitation in electrically driven ships by acting on the motor speed reference was proposed by S.-Y. Kim et al. [43]. An ample and interesting review on electrified waterborne mobility has recently been published by Qazi et al. [44], which highlights onboard and dock challenges and identifies power electronics as a key enabling technologies in tackling the several challenges toward a reliable maritime transport.

As regards small vessels, a study for the design of a small all-electric passenger boat was proposed by Postiglione et al. [45], while a comparative analyses of different propulsion schemes suitable for waterbuses in Venice was presented by Guarnieri et al. [46]. The study on the optimal management of the power flows in a hybrid storage system made of battery and supercapacitor intended for a Venice waterbus is presented in [47]. Another study on a hybrid diesel-electric powertrain intended for a Venice waterbus comparing series and parallel hybrid architectures and focused on emission abatement is described in [48]. However, all previous papers report on numerical simulations of hybrid electric powertrains, not followed by a real prototypes or pilot boats, and in some cases the model presented are affected by major flaws which induce some doubt on the validity of the reported results. Differently, the simulation of a full electric hybrid fuel cell/battery system for a really built small boat (peak power of 110 kW) aimed at analyzing the system dynamics and its management is presented in [49], but it leaves some doubt on how the battery is interfaced to the boat busbar and how the battery state of charge is controlled.

4.2. Specifications and architecture choice

The design of the prototype vessel was developed on the ground of the knowledge acquired from the literature cited above and of the specifications imposed by Veritas with the aim of fostering a smooth introduction of the electrical propulsion in the company technological know-how and infrastructure. In detail, it was required.

- to preserve the ICE boat navigability and maneuverability in the twisting and narrow routes,
- to preserve the ICE boat operability in daily waste-collecting service,
- to eliminate emissions and minimize noise in the in all routes inside the historical city (e.g., Cannaregio and Giudecca of Table 1) and minimize emissions and noise elsewhere (e.g., Castello, Murano and Island, of Table 1),
- to maintain onboard powered services (propulsion, caisson compactor, crane, cockpit, …),
- to eliminate onboard mineral-oil hydraulic circuits, thus getting rid of leakage risks,
- to adopt commercial devices and share as many components as possible with standard ICE boats and to be driven and maintained by the same crew skilled on standard boats, to achieve best interoperability with existing vessels,
- to comply with the tight (and often obsolete) regulations of the Italian water authorities, notably imposing redundant power sources but allowing a single propulsor.

Direct consequences of these specifications were the following requirements.

- to maintain the 12-m hull and external sizes of ICE boats and the 360°azimuthal propulsion,
- to maintain the onboard waste caisson that occupies a large part of the hull,
- to navigate full electric in all city center routes and to use possibly a thermal engine only along few outer routes.

The previous specifications and requirements strongly limited the onboard space for hosting the powertrain and all power drives. Some alternative solutions derived from the literature were investigated, demonstrating that most of them were not or hardly viable. Notably.

- a parallel hybrid system would involve a double-powered azimuthal propulsor, too cumbersome to find place in the space available onboard;
- a full-electric battery-powered system recharged only at the docking station would require a battery too large to be allocated onboard whereas en-route recharging stations remained unavailable;
- a full-electric hybrid system powered by a fuel-cell and a battery or supercapacitor could be adopted, but it raised operativity issues because at present a hydrogen refueling station is missing in Venice. However, Veritas plans to develop such a prototype in the future.

Consequently, a battery series hybrid powertrain was chosen by the designers, hence the name Plug-in Hybrid Electric Boat One (PHEB1), in which a battery powers all onboard power drives (two of them via water hydraulic circuits) in normal navigation and a small diesel generator (DG) flanks the battery working as a *range extender* only on longer routes outside the city center (Fig. 4), so that a full-electric zero-emission service is ensured in the city center.

With respect to a full-battery vessel capable of the same services, this plug-in series hybrid architecture, which has been successfully adopted in other similar-size boats [50], requires a smaller battery than a full electric boat, that can fit in the tight spaces unoccupied by cockpit, crane, and caisson inside the hull. Compared to the diesel ICE of conventional vessels, the *range extender* DG is smaller and is operated only in case of low battery State of Charge (*SOC*) at a steady-state high-efficiency working point. Consequently, PHEB1 presents a higher

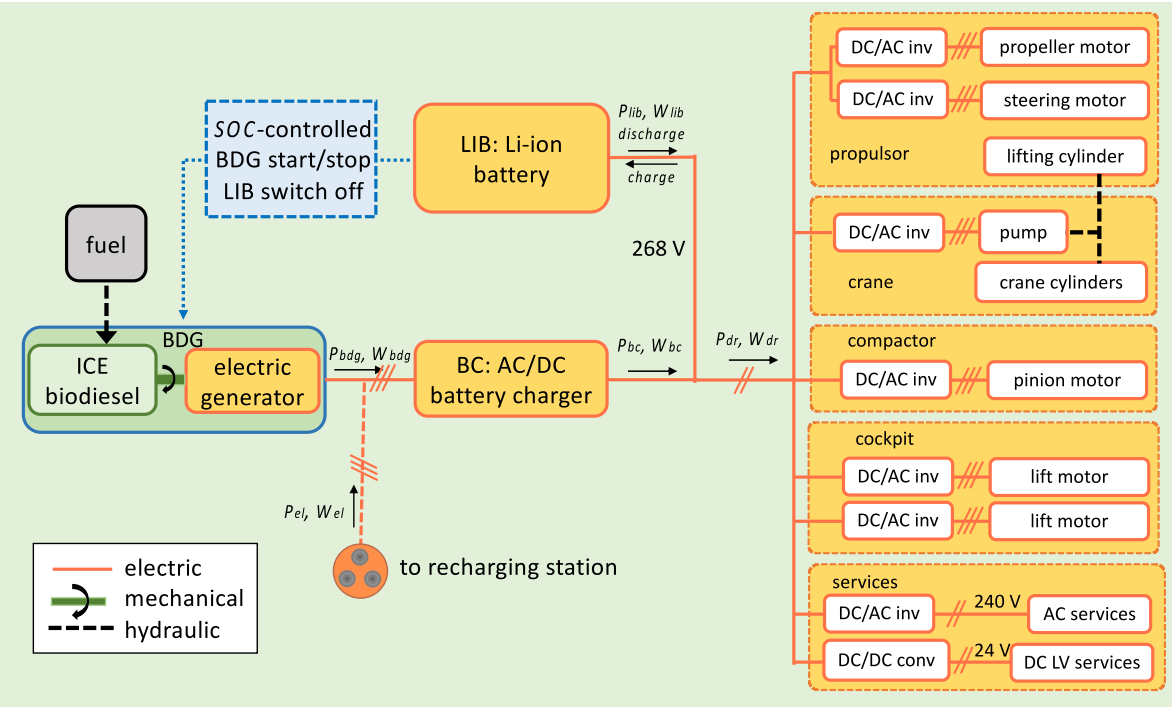

Fig. 4. The LIB-BDG series hybrid powertrain architecture adopted in PHEB1. Normally the lithium-ion battery (LIB) powers all electric drives (propeller, steering, compactor, crane, and other services). A small biodiesel generator (BDG, made of an ICE and an electric generator) coupled to a battery charger (BC) operates as a *range extender* that recharges the LIB anytime its state of charge (*SOC*) drops low.

efficiency than conventional ICE boats [51,52]. In addition, the DG may power the boat drives alone in the event of a battery failure or full discharge, thus providing the redundancy required by navigation regulations, that is mandatory also in internal waters. The adopted series hybrid scheme induced some design choices (Fig. 5). Given the reliable products and components for electric and hybrid vehicles available on market, it was chosen to optimize such product and components matching in a technology integration approach. Compared to the existing literature, PHEB1 presents an unparalleled complex powertrain and drive configuration for its size. In addition, almost all literature consists of theoretical studies and basic designs. Conversely, we developed a basic design, executive design, construction and operation of the real boat, including its on-field experimental validation.

4.3. System design: powertrain and drives

The sizing of the components and drives was made to comply with the performance and operations of the existing ICE boats, so as to

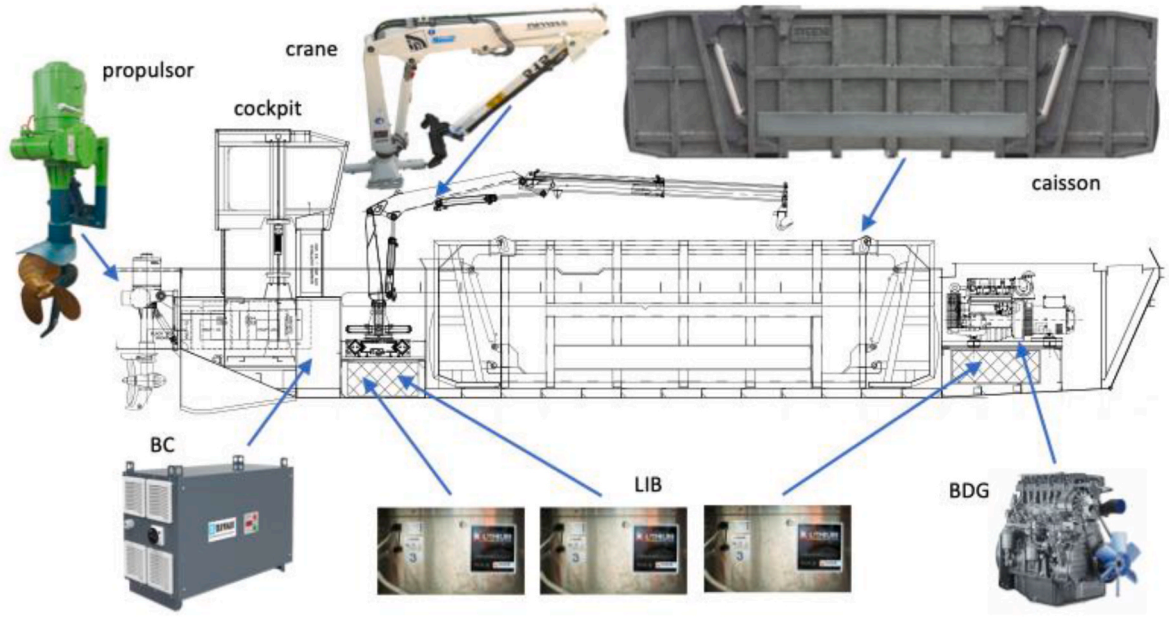

Fig. 5. Sketch of PHEB1, with the layout of the power units (power supplies and power drives): azimuthal propulsor, collapsible cockpit, crane, caisson, battery charger (BC), Li-ion battery (LIB) in three modules, and biodiesel generator (BDG).

provide the same services along the routes, while saving costs and emissions. Series products of specialized manufactured were selected after extensive technical discussions and testing.

4.3.1. Battery

At present, Li-ion are the chemistries of choice for mobility applications. Different types of Li-ion cells, with various cathodic materials, were compared in terms of specific power P_s [W/L] and energy E_s [Wh/L], and power P_d [W/kg] and energy E_d [Wh/kg] densities, as well as of life cycles, operation reliability and hazard resilience. Cells using Cobalt were excluded, notably Lithium Nickel Cobalt Aluminum Oxide ($LiNi_xCo_yAl_zO_2$ – NCA) and Lithium Nickel Manganese Cobalt Oxides ($LiNiMnCoO_2$ – NMC), despite their higher energy density and wide success in electric vehicles, due to ethical concerns on manpower exploitation and child labor in mining activities, particularly in the Democratic Republic of the Congo where Cobalt minerals are mostly mined [53–55]. Some ethical concerns arise also from Lithium mining, but to a minor extent and commercial non-lithium cell perform much less so that they had to be excluded [56,57], while more advanced chemistries are not yet ready for market exploitation [58]. The final choice has been Lithium Iron Phosphate ($LiFePO_4$ – LFP), whose cells typically present E_s = 220–325 Wh/L, about 25% less than Cobalt type Li-ion cells but are also less prone to thermal runaway. When referred to a whole battery module the specific energy typically drops to 80–90 Wh/L. Based on these values and the space available onboard, the deliverable work of the Lithium-ion Battery (LIB) was set by rounding off the maximum boat drive demand over routes inside the city center (i.e., Canareggio, Giudecca, Castello routes of Table 1):

$$W_{del} = 64 \text{ kWh} \tag{3}$$

Indeed, electric drives made of an inverter and an electric motor have higher efficiency than hydraulic motors and thus require a lower input power to deliver the same mechanical work. Notably, electric drives of the size here considered reach efficiencies of 88%–94% against 75%–82% of equivalent hydraulic motors installed in the Veritas ICE boat, so that a reduction of the work demand around 14% can be expected after electrification. However, the same work demand of the hydraulic drives was prudentially considered, to account for possible extra discharge losses, extra demand and capacity loss (e.g. after aging [59]). The LIB nominal energy E_{lib} was determined as:

$$E_{lib} = W_{del}/DOD = 80 \text{ kWh} \tag{4}$$

For the depth of discharge a DOD = 80% has been assumed, as typically specified by manufacturers. The battery gross volume was estimated in 850–950 L. To achieve this battery rating three commercial modules were selected, each made of 28 series-connected $LiFePO_4$ 3.2-V 300-Ah cells. These three modules were also connected in series to form a battery rated 268 V 300 Ah 80.6 kWh, delivering a steady-state power of 70 kW and weighting 1125 kg. Each module is provided with a Battery Management System (BMS) including two thermal sensor per cell and providing fast active/passive cell rebalancing to counteract single performance drift and possible thermal runaway. Two modules are placed under the crane and one under the DG. The main parameters of the selected battery are reported in Table 2.

The LFP battery voltage in discharge was predicted by means of an adaptation of the SOC-dependent Shephard model [60]:

$$V_{lib} = N\left\{V_{co} + A_c\, exp[-B_c(1-SOC)] - K_v\frac{Q}{SOC}(1-SOC) - \frac{K_r}{SOC}\, i^* - R_{ic}\, i\right\} \tag{5}$$

where N is the total number of cells in series, V_{co} [V] is the constant term of the open circuit voltage, A_c [V] and B_c [−] are two empirical constants, K_v [Ω s^{-1}] is the cell polarization overvoltage coefficient, K_r [Ω] is the polarization resistance coefficient, SOC is the state of charge, i [A] the current and i^* its low-pass filtered value, and R_{ic} [Ω] the constant part of the cell internal resistance. This model was proved to reproduce quite accurately the electric behavior of Li-ion battery, and a small adaptation allows to represent the cell behavior in charge [61]. The last three terms in braces account for cell losses. The parameters for the adopted $LiFePO_4$ cell are indicated in Table 3. The voltage of eq. (5) is provided by the equivalent circuit of Fig. 6. A full dynamic equivalent circuit for Li-ion cells would include also one or two R-C loops, modeling fast time responses. Since the dynamic times of the electric drive profiles are slower, in the order of a fractions of second, such R-C loops have not been considered in the equivalent circuit here adopted

Table 2
Selected battery main parameters (from manufacture's datasheet).

Symbol	Parameter	Unit	Value
E_{lib}	Rated energy	kWh	80.6
V_{lib}	Rated voltage	V	268
Q_{lib}	Rated capacity	Ah	300
$P_{lib\text{-}rated}$	Rated power (steady state)	kW	70
$P_{lib\text{-}peak}$	Peak power (10 s)	kW	80
N_m	Number of modules in series	–	3
N_{cell}	Number of cells in series per module	–	28
N_p	Number of cells in parallel per module	–	1
R_i	Cell internal resistance	mΩ	0.4
–	Module size L × P × H	mm	1000 × 783 × 383
w_m	Module weight	kg	375
IP	IP grading	–	IP65
T_{op}	Operating temperature	°C	−15 to +45
LC	Life cycle at DOD = 80 %	cycles	2000

4.3.2. Power and service busbars

The battery is directly connected to the power busbar, setting its voltage at 268 V DC, where also the DG and all power drives are connected. In addition, the power busbar feeds two service busbars, one single phase AC and one low voltage DC, through a 268–240-V DC/AC inverter and a 268–24-V DC/DC converter, respectively. These service busbars supply the low power services described in Section 4.3.10.

4.3.3. Biodiesel generator

The DG, to be used as a range extender, has been sized at a rated power of 20 kW and has been specified to work on biodiesel (BDG), in compliance with the company emission reduction policies. The adopted BDG was a 4-cylinder turbo engine coupled with a generator delivering 19.4 kW AC three-phase at 400 V 50 Hz that presents the best efficiency among similar models running on biodiesel. It has been located at the vessel bow.

4.3.4. Azimuthal propulsor

The azimuthal propulsor has been powered by two electric motors, i.e. a 50-kW permanent-magnet synchronous motor (PMSM) driving a three-blade propeller and a 5-kW PMSM driving a 360° steering. An electrically pressurized hydraulic cylinder hoists the whole propulsor for shallow water navigation and in-service propeller maintenance. The PMSMs are controlled by variable-frequency drives (VFDs) consisting of DC-AC three-phase encoder-feedback-controlled inverters fed from the 268-V DC busbar. They perform advanced flux-vector control that ensure precise control of torque-speed characteristics for thrust and steering, resulting in high maneuverability and ease of operation. Since electric motors rotate in both directions, the electric prolusion has no mechanical rotation reverser, resulting in higher efficiency, simpler propeller control, very low noise, and reduced maintenance.

Table 3
Parameters for the $LiFePO_4$ cell model of eq. (5) taken from Ref. [61].

V_{oc} [V]	A_c [V]	B_c [−]	K_v [Ω s^{-1}]	K_r [Ω]	R_{ic} [mΩ]
3.25	0.2642	61.062	5.7 10^{-5}	5.7 10^{-5}	0.285

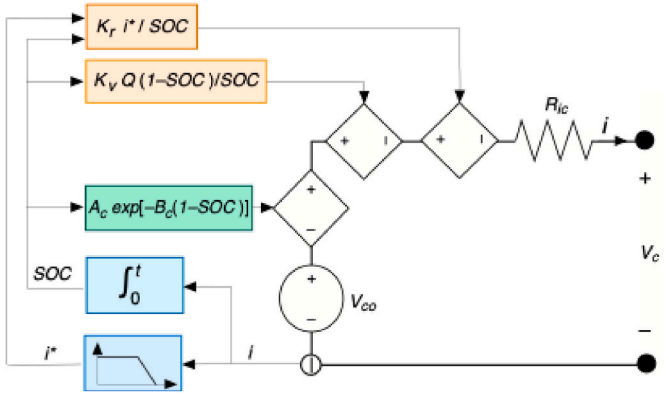

Fig. 6. Equivalent circuit of the $LiFePO_4$ cell modeled in eq. (5).

4.3.5. Caisson and compactor

The 18.8 m^3 caisson preserved the size, shape, and layout of the standard ICE vessels, but the hydraulic cylinders operating the compactor were replaced with two rack-and-pinion mechanisms, one on each side, moving the double-room compactor. The pinions are driven by a 50-kW PMSM through a VFD DC-AC three-phase encoder-feedback-controlled inverter fed from the 268-V DC busbar. It provides advanced flux-vector control to ensure smooth kinematic and reduced noise.

4.3.6. Crane

Extensive investigations showed that electrifying the crane five movements would require cumbersome and costly electric drives and a new crane design. It has been preferred to maintain the original 4-jig 5-drive 4.5-m 250-kg hydraulic crane. However, to get rid of oil shedding risk, hydraulic cylinders working on purified water were adopted. Water is pressurized in a dedicated tank by a 10-kW electric pump fed from the 268-V DC busbar through a dedicated controller.

4.3.7. Collapsible cockpit

The cockpit collapsing mechanism uses two fixed vertical worms, one at each side, each hosting the hollow threaded shaft of a 1-kW electric motor mounted onto the cockpit, that is fed from the busbar through a dedicated controller. When the shafts rotate the motors travel along the worm, hauling the cockpit, while two rails on each side provide guidance.

4.3.8. Battery charger and Power Managements Systems

Except the LIB that is directly connected to the busbar, all other power units (BDG and power drives) are connected to the power busbar via Power Managements Systems (PMSs), namely electronic devices ensuring effective operation [62]. The BDG PMS is a commercial unidirectional battery charger (BC) made of a three-phase AC/DC uncontrolled converter in cascade to a DC/DC isolated bridge converter (including a 20 kHz transformer, Fig. 7a). The single-phase equivalent circuit is shown in Fig. 7b, where $L = 3.5$ mH and $R = 1.75$ Ω. It delivers 15.4-kW DC power when supplied with 18 kW AC three-phase at a power factor of 0.94, by the BGD. During routing, it controls the BDG power flow to the power busbar to provide vessel range extension. It also performs the full LIB recharge after service, from a 15 kW/400 V three-phase AC charging station in the Veritas dock, at lower cost and emissions than the BDG. The BC controls a constant current (C/4.9 rate) + constant voltage (galvanostatic/potentiostatic) profile to reach 100% SOC, as sketched in Fig. 7c.

Each power drive is interconnected to the 268 V power busbar through a PMS made with a commercial unidirectional inverter controlling the required power profile, given that no regenerative operation (i.e. energy recovery) is possible. Some details of the propulsor and caisson PMSs have been given above. Table 4 lists all Power Units with

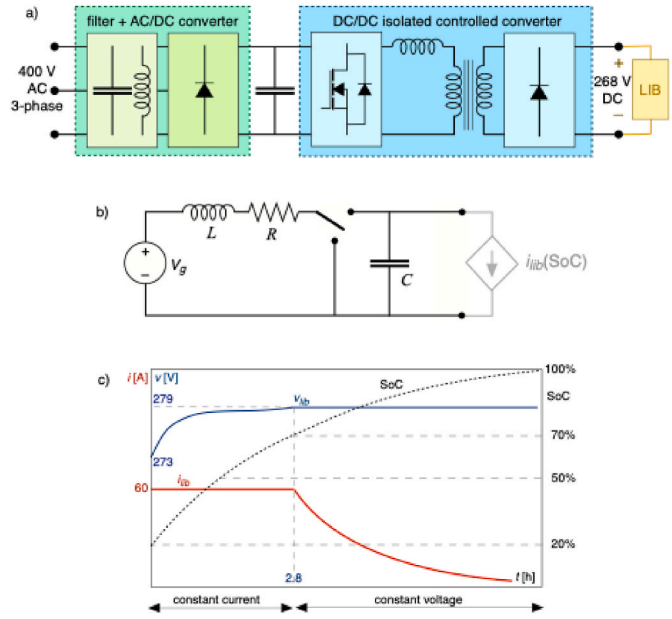

Fig. 7. Battery charger: a) electric scheme; b) single-phase equivalent circuit; c) constant-current-constant-voltage (CC-CV) charging protocol to reach *SOC* = 100%.

their respective PMSs, summarizing their main data, consisting of the Power Unit rated power [kW] and rated voltage [V] the electric conversion operated by its PMS, the PMS rated power and the type of control performed on the PMS. In particular, propeller, steering and compactor use PMSs of the variable-frequency driver (VFD) type and the cockpit screw-drives use insulated-gate bipolar transistor (IGBT) drives. These PMSs have been selected to ensure that the supplied power equates dynamically the mechanical drive power demand. Slight oscillations in the power input possibly deriving from the proportional-integrative-derivative (PID) control setting do not undermine the stability of the drives thanks to the much shorter duration of electronic-electric response (ms) with respect to characteristics drive mechanical times (hundreds of ms).

4.3.9. Dashboard

The dashboard inside the cockpit includes a human machine interface (HMI) made with a touch-screen monitor allowing the operator to drive the boat while monitoring data from GPS and radar, as well as to operate the crane, the compactor, and the cockpit. Instrumentation includes navigational tools and radio.

4.3.10. Low power services

On-board services are both 240 V AC and 24 V DC, fed from the respective busbars. The former include cockpit conditioner, inverter cooling pump, and service socket. The latter comprise a 24 V battery, bilge pump, navigation lighting, horn, windscreen wiper, radar, radio, GPS, and service socket.

4.4. Energy management system – EMS

4.4.1. Targets and strategies

The Energy Management System (EMS) is the brain of a boat power system and controls how the energy sources contribute to supply the onboard drives. It receives signals from the power units, such as the drive power demands and the battery *SOC*, and evaluates the actions needed to control the power flows. Basically, the EMS performs this power flow management by operating switches of a switchboard that connects the power sources to the busbar and the drives and by controlling the level of power delivered to each drive by acting its PMSs.

Table 4
Main data of all power devices connected to the 268 V DC busbar: Power Units (LIB, BDG and electric drives) with rated power and voltage; respective power management systems (PMSs) with electric conversion type, hardware type, power rating and control type.

Power Units:supplies or power drives			Power Managements System – PMS			
Type/function	**P_{pu} [kW]**	**V_{pu} [V]**	**Conversion**	**Hardware**	**P_{pms} [kW]**	**Control**
$LiFePO_4$ battery	70–80	268 DC	–	direct connection to busbar	80–70	–
BDG	19.4	400 AC	three-phase	controlled converter	15.4	EMS/operator
– grid			AC/DC			
Propeller PMSM	50	295 AC	DC/AC three-phase	VFD flux-vector encoder feedback-controlled inverter	60–100	Operator
Steering PMSM	5	295 AC	DC/AC three-phase	VFD flux-vector encoder feedback-controlled inverter	15	Operator
Compactor PMSM	50	295 AC	DC/AC three-phase	VFD flux-vector encoder feedback-controlled inverter	60–100	Operator
Crane pump PMSM	10	295 AC	DC/AC three-phase	AC flux-vector encoder feedback-controlled inverter	25	Automatic
n.2 Cockpit PMSM	1	240 AC	DC/AC three-phase	IGBT-based PWM Digital AC motor controller	1–2	Operator

Table 5
Rule-based EMS control. The different LIB states depend of the LIB *SOC*, which automatically triggers the BDG on (when $SOC \leq 35\%$), LIB charge only (when $SOC \leq 20\%$) and BDG off (when $SOC \geq 90\%$). To do so, the EMS status to $S_{ems} = 0$–1–2, setting the BDG switch $S_{bdg} = 0$ (off) or 1 (on) and the charge only conditions of the LIB.

LIB *SOC* and BDG status		EMS S_{ems}	S_{bdg}	BDG	LIB state	Power flow
$35\% \leq SOC \leq 100\%$	BDG off	0	0	off	discharge	$P_{dr} = P_{lib}$
$SOC \leq 35\%$	BDG off	$0 \rightarrow 1$	$0 \rightarrow 1$	off → on		
$20\% \leq SOC \leq 90\%$	BDG on	1	1	on	charge/ discharge	$P_{dr} = P_{lib} + P_{bdg}$
$SOC \leq 20\%$	BDG on	$1 \rightarrow 2$	1	on		
$20\% \leq SOC \leq 35\%$	BDG on	2	1	on	charge only	$P_{dr} - P_{bdg} = P_{lib} \leq 0$
$35\% \leq SOC$	BDG on	$2 \rightarrow 1$	1	on		
$35\% \leq SOC \leq 90\%$	BDG on	1	1	on	charge/ discharge	$P_{dr} = P_{lib} + P_{bdg}$
$90\% \leq SOC$	BDG on	$1 \rightarrow 0$	$1 \rightarrow 0$	on → off	discharge	
$35\% \leq SOC \leq 90\%$	BDG off	0	0	off	discharge	$P_{dr} = P_{lib}$

These actions can be based on different strategies, which characterize different types of EMSs. Very often these strategies consist in some optimization algorithm. Some examples are: maximization of energy efficiency [49]; minimization of the overall energy or equivalent fuel consumption [40]; minimization of the battery size and cost [63]. Some EMS can pursue the optimization of more performance parameters at the same time, by executing a multi-objective strategy. Alternatively, the vessel can be operated on the base of predefined rules, in which case the strategy consists in a series of coded instructions. In any case, high battery DODs must be avoided to prevent premature degradation [64]. Some examples of EMSs performing such strategies are classical proportional integral [65,66], dynamic programming [67], fuzzy logic [68], charge-depleting charge-sustaining (CDCS) [69], Equivalent fuel consumption minimization strategy (ECMS) [70], state based (or rule based) [40,49], multi-scheme (i.e. a combination of the previous) [71].

4.4.2. PHEB1 state-based EMS

The PHEB1 prototype has been provided with a rule-based EMS, consisting of a series of coded instructions which define the actions and the power flow in each possible operational mode at different battery *SOC*. These instructions implement the vessel hybrid series mode which consists in keeping the LIB normally (i.e. as far as $SOC > 20\%$) powering all power drives and in using the BDG as range extender, i.e. recharging and supporting the LIB in case of low *SOC* (i.e. if $SOC \leq 35\%$) due to prolonged routing. The BDG can also be operated as emergency power supply, although at reduced power, in the case of extreme low *SOC* (i.e. $SOC \leq 20\%$) or LIB fault. To do so, the EMS can assume three different states $S_{ems} = 0$–1–2, depending on the *SOC* and the BDG state, which switch the BDG mode $S_{bdg} = 0$ (off) or 1 (on) and the LIB charge only conditions, as synthetized in Table 5. Initially the BDG is turned off and the LIB supplies the total drive power P_{dr} (EMS state $S_{ems} = 0$). The BDG is turned on at full power P_{bdg} when the LIB *SOC* drops to the lower threshold $SOC_{low} = 35\%$ ($S_{ems} = 0 \rightarrow 1$, $S_{bdg} = 0 \rightarrow 1$) and in this state, depending on the sign of $P_{bdg} - P_{dr}$, the LIB recharges or discharges at a reduced rate while the drives are still supplied at full power (70 kW steady state). The LIB can only recharge if *SOC* drops to $SOC_{min} = 20\%$ ($S_{ems} = 1 \rightarrow 2$, $S_{bdg} = 1$). If the LIB *SOC* recharges above $SOC = 35\%$ it goes back to normal operation ($S_{ems} = 2 \rightarrow 1$, $S_{bdg} = 1$). The BDG is turned off in the case the *SOC* reaches the upper threshold $SOC_{up} = 90\%$ ($S_{ems} = 1 \rightarrow 0$) because this level of charge is enough for the boat to complete the route and go back to the dock powered only by the LIB. Full recharge is completed from the grid at the dock recharging station, at lower cost and emissions.

4.5. Servicing simulations

4.5.1. Work flow model

The rationale of the *range extender* architecture is to operate as much as possible PHEB1 in full electric mode powered by the LIB to ensure no pollution in the fragile historical heritage of Venice city. However, in the design phase it was verified what would be the effects of this EMS strategy on the overall work consumption and operating costs. To this aim, a model was implemented estimating the fuel consumption and energy operating cost of PHEB1 along two routes: Giudecca (full electric mode) and Islands (range-extender hybrid mode). Although this paper is more focused on the design choices and construction, a brief description of the model and its results is given hereafter.

The boat power sources were the LIB (Section 4.3.1) and the BDG through the AC/DC battery charger (Sections 4.3.3 and 4.3.8) controlled by the state-based EMS (Section 4.4.2). Since an accurate analysis of the mechanics and dynamics of propeller, steering, compactor, crane and cockpit were not required in these simulations, all power drives profiles were modeled as a single load absorbing the net total power $P_{dr}(t)$ that had been measured in the preliminary experimental campaign with an ICE vessel on the two routes (Section 3). This was a prudential assumption because the efficiency of electric drives is noticeably higher than that of hydraulic drives so that they absorb a lower power to provide the same service. For example, Bruzzese et al. [72] compared hydraulic and electric drives for the same service, reporting efficiencies of 51.7% and 79.7%, respectively. The energy $E_{lib}(t)$ stored in the battery during servicing ($0 \leq t \leq T$) and the corresponding $SOC(t)$ were computed as the initial full energy less the consumed in all drives and

internal LIB losses, plus the net energy released by battery charger:

$$E_{lib}(t) = E_{lib}(0) - \int_0^t [P_{dr}(t') + P_{lib.ls}(t')]\, dt' + \int_0^t S_{bdg}\, [P_{bdg} - P_{bdg.ls}(t')]\, dt' \quad (6)$$

$$SOC(t) = E_{lib}(t) / E_{lib}(0) \quad (7)$$

where $E_{lib}(0) = 80.6$ kWh is the energy initially stored in the LIB at $SOC(0) = 100\%$ (Table 2), $P_{lib\text{-}sl}(t)$ is the power lost in the LIB according to the model of eq. (5). $P_{bdg} = 18$ kW is electric power delivered by the BDG to the AC/DC battery charger (BC), equal to the BC rated power, and $P_{bdg.ls}$ is the power lost therein according to the equivalent circuit of Fig. 7b. S_{bdg} is the BDG state switch controlled by the EMS protocols of Table 5, that is initially $S_{bdg} = 0$ (BDG off), switches to $S_{bdg} = 1$ (BDG on) when the SOC reduces at the lower threshold $SOC_{low} = 35\%$, and switches again to $S_{bdg} = 0$ (BDG off) whenever the SOC rises back to the upper threshold $SOC_{up} = 90\%$. Eq. (6) calculates the present energy stored in the LIB by subtracting from its initially stored energy the work consumed by all drives at the net of LIB internal losses and adding the work supplied by the BDG at the net of its internal losses. Depending on the values of the two integrals in eq. (6), $E_{lib}(t)$ may decrease or increase. Eq. (7) calculates the LIB SOC as ratio between the present stored energy and the rated energy.

The BDG total delivered work W_{bdg} and consumed biodiesel volume V_{bd} were computed as:

$$W_{bdg} = \int_0^T S_{bdg}\, P_{bdg}\, dt' \quad (8)$$

$$V_{bd} = \frac{1}{NCV_{bd}\, \rho_{bd}} \int_0^T \frac{S_{bdg}\, P_{bdg}}{\eta_{bdg}}\, dt' \quad (9)$$

where T is the route duration, $NCV_{bd} = 10.35$ kWh kg^{-1} is the biodiesel net calorific value and $\rho_{bd} = 0.88$ kg L^{-1} its density. The BDG efficiency η_{bdg} profile was deduced from the ICE brake-specific fuel consumption (i.e. gravimetric fuel consumption) values tabled by the manufacturer at different loads, obtaining a value $\eta_{bdg} = 31.8\%$ at 18 kW, slightly higher than the value 31.5% at full power. The electric work W_{el} supplied by the charging station to recharge the LIB through the AC/DC battery charge according to the CC-CV protocol of Fig. 7c was computed as:

$$W_{el} = [E_{lib}(0) - E_{lib}(T)] + \int_0^{T_{ch}} [P_{lib.l}(t) + P_{bc.l}(t)]\, dt \quad (10)$$

The total cost for the consumed energy was obtained as:

$$C_{tot} = C_{bd} + C_{el} = V_{bd}\, p_{bd} + W_{el}\, p_{el} \quad (11)$$

from the prices of the fuel $p_{bd} = 0.785$ € L^{-1} and electricity $p_{el} = 0.248$ € kWh^{-1} paid by Veritas in 2023, the latter being the reduced price paid as a public utility company.

The parameter values used in the computation are summarized in Table 6. The computed values of burnt biodiesel V_{bd} (resulting in local emissions) and energy costs C_{tot} were compared with the measured quantity V_{ice} (Table 1) and cost $C_{ice} = V_{ice}\, p_{bd}$ of the biodiesel burnt in the present ICE boat.

Table 6
Additional parameters used in the model simulations.

Symbol	Parameter	Unit	Value
SOC_{low}	SOC lower threshold (BDG ON)	–	35%
SOC_{min}	SOC minimal threshold to (LIB OFF)	–	20%
SOC_{up}	SOC upper threshold (BDG OFF)	–	90%
NCV_{bd}	Biodiesel net calorific value	kWh kg^{-1}	10.35
ρ_{bd}	Biodiesel density	kg L^{-1}	0.88
η_{bdg}	Biodiesel generator efficiency at 18 kW output power	–	31.8%
p_{el}	Electricity price	€ kWh^{-1}	0.248
p_{bd}	Biodiesel price (public utility companies only)	€ L^{-1}	0.785

4.5.2. Full-electric mode simulation

Simulation results in the Giudecca route showed that the LIB alone was able to meet the load power profile and the peak power demand of 67.5 kW, consistently with the electric response time <1 ms much shorter than the ICE + hydraulic response time. The LIB delivered the whole work demand $W_{del} = W_{dr} = 46.2$ kWh and the BDG was never turned on, thus servicing in a full-electric zero-emission mode. The stored energy at the end of the route was $E_{lib}(T) = 32.2$ kWh ($SOC = 39.9\%$) and recharging the battery from the grid required an electric work $W_{el} = 59.3$ kWh costing 14.74 €. No fuel was burnt against 28.4 L needed by an ICE boat on the same service, costing 22.3 €. The relative saving in cost and locally burnt fuel were $S_{cost} = 34.0\%$ and $S_{bd} = 100.0\%$, with a total abatement of emissions.

4.5.3. Hybrid mode simulation

Simulation results in the Islands route showed that the battery was always able to meet the load power profile and the peak power demand of 64.3 kW but it could not provide the whole work $W_{dr} = 103.1$ kWh. When SOC reduced to 35% the BDG was turned on to operate in a hybrid range extender mode reducing the LIB discharge rate. At the end of the route the LIB had delivered $W_{del} = 60.8$ kWh and its SOC had reached 20.9% while the BDG had delivered 42.3 kWh working on almost 3 h and consuming 14.6 L of fuel that cost 11.5 €. Recharging the battery from the grid required an electric work $W_{el} = 78.1$ kWh paid 19.4 €. The total cost was 30.83 €, against 48.6 L and 38.1 € needed by an ICE boat on the same service, with relative savings $S_{bd} = 70.0\%$ and $S_{cost} = 19.2\%$, respectively, and with a substantial reduction of emissions.

The results obtained in the simulations of the two routes are summarized in Table 7, where W_{dr} is the work consumed by all drives; V_{ice}, C_{ice} are the volume and cost of fuel consumed by the ICE boat; W_{del} is the work delivered by the LIB of PHEB1; W_{el} is the work needed to recharge the LIB from the grid at the end of routing; W_{bdg} is the work delivered by the BDG; V_{bd} is the volume of fuel consumed by the BDG; C_{tot} is the cost of fuel and electricity consumed by PHEB1; S_{bd} is the relative saving in fuel (i.e. emissions) allowed by PHEB1; S_{cost} is the relative saving in energy cost allowed by PHEB1. Simulations showed a reduction of burnt fuel (i.e. emissions) of 100 % in the pure electric Giudecca route and of 70% in the hybrid electric Islands route. The corresponding cost savings were 34% and 19.2%, respectively.

Although the simulations regarded only the energy operational costs, they indicated significant economic and emission advantages of the electric propulsion on the conventional ICE, confirming the profitability of the design. A more complete comparison would include all operative and capital costs to be accounted in a levelized cost of energy (LCOE)

Table 7
Model simulated results: work, fuel consumption and energy costs in Giudecca and Islands routing with ICE vessel and PHEB1. Computed values showed a 34% saving in energy cost and 100% saving in fuel in the Giudecca route for PHEB1 compared to the ICE vessel. In the case of the Islands route (longer) savings were respectively 19.2% and 70%.

Item	Unit	Giudecca route (short)		Islands route (long)	
		ICE boat	PHEB1	ICE boat	PHEB1
W_{dr}	kWh	46.20	46.20	103.1	103.1
V_{ice}	L	28.41	0	48.58	0
C_{ice}	€	22.31	0	38.14	0
W_{del}	kWh	0	46.2	0	60.83
W_{el}	kWh	0	59.34	0	78.13
W_{bdg}	kWh	0	0	0	42.27
V_{bd}	L	0	0	0	14.59
C_{tot}	€	0	14.72	0	30.83
S_{bd}	–	–	100%	–	70.0%
S_{cost}	–	–	34.0%	–	19.2%

analysis, whereas a life cycle assessment (LCA) would take into account the costs and emissions in all stages of the vessel life, from raw material provision to end-use disposal and recycling. For the sake of example, greenhouse gas emission in the production of Li-ion battery is estimated to equal approximately 200 kg CO_2eq/kWh [73], but this figure was found to weight as 2.7% of the emission reduction achieved with hybrid electric powertrains over the battery life [63], showing that electric propulsion remains profitable in terms emission abatement even when battery manufacturing emission are taken into account, in view of a life cycle assessment (LCA). This data indicates that, even considering the emissions due to Li-ion manufacturing, the substitution of the ICE boats with hybrid electric boats is beneficial in terms of total emission (manufacturing plus operation). However, deepening this aspect of the analyses is out of the scope of the present work and is left to future investigations.

5. Regulations, shipbuilding and operation

5.1. Regulations and shipbuilding

As PHEB1 was intended to navigate in internal waters, authorizations by three authorities had to be obtained, namely RINA (the operative branch of the Italian Maritime Registry), Venice Port Authority and Port Inspectorate. Unfortunately, up-to-date standards for full electric and hybrid vessels as well as for internal water vessels have not yet been issued in Italy and authorities follow often obsolete standards, usually according to strict interpretations. RINA imposed that the main motor formally had to be an ICE and the LIB full electric mode had to be classified as emergency. This was a major reason to implement the redundant propulsion scheme in the EMS, with the powertrain powered by the BDG and the LIB disconnected.

More generally, RINA imposed full redundancy of the powertrain including navigation drives, inverters, and electronic control systems, except propeller and its electric motor. On the one hand this redundancy ensured a high level of reliability, but on the other hand it increased capital expenditure (CAPEX), complexity and failure probability. PHEB1

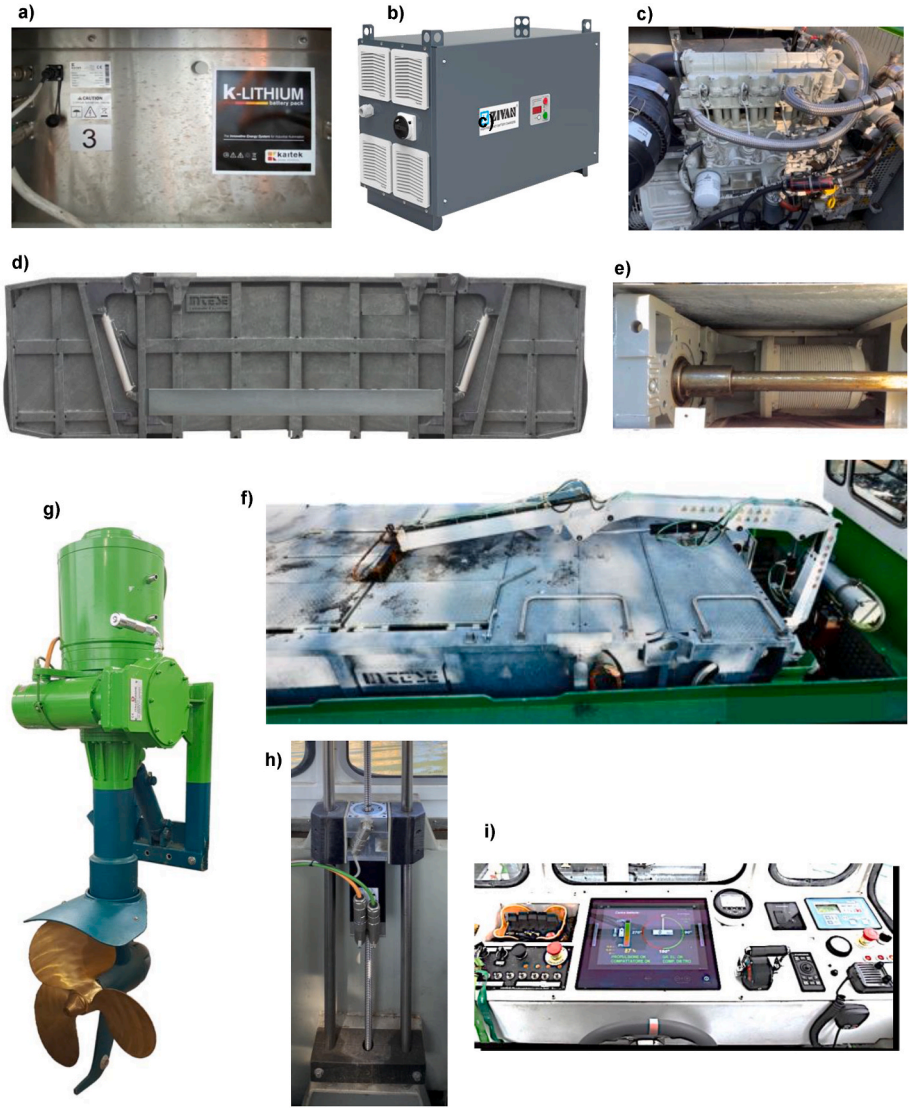

Fig. 8. Components of the PHEB1 (not in scale). a) One of the three modules forming the $LiFePO_4$ battery by Flash Battery (I); b) 15.4 kW battery charger by Zivan (I); c) Biodiesel generator: 19.4 kW F3M2011 by Deutz (D); d) Waste caisson (lateral view) with e) motor of the two-way compactor (back view); f) Crane laid on the caisson: capable of five movements driven by hydraulic pistons; g) Propulsor: azimuthal IGP-75-01200 by Italdraghe (I); h) Collapsing cockpit: right-hand side drive moving with the cockpit along a worm; i) Dashboard with HMI touch-screen monitor (center), and boat controllers.

Fig. 9. Launching PHEB1.

was built by a local shipyard according to the design outlined here. Fig. 8 shows pictures of its installed components and Fig. 9 its launch. It is not an exaggeration stating that the most difficult hurdles in design and shipbuilding derived from regulations constraints rather than from technical challenges.

5.2. Commissioning tests

Commissioning started after all authority permissions were released. The first test phase consisted in tuning-up and adjusting some functionalities, particularly in the EMS logic and wiring. The second test phase consisted in operating the boat in real service along usual routes. Pilots training just needed a few-hour to familiarize with the electric powertrain and its control, thanks to the ease of use and user-friendly HMI (Fig. 10). Operations along short and long routes allowed to test the boat in full electric mode and range-extender hybrid mode, respectively. Short routes, such as Cannaregio and Giudecca of Table 1, were driven in full electric mode. The LIB initial $SOC(0)$ and final $SOC(T)$ states of charge were given by the BMS of the LIB modules and allowed to compute the LIB net energy consumption as $W_{lib} = [SOC(0) - SOC(T)]$ $E_{lib}(0)$ while the refueling biodiesel volume V_{bd} allowed to compute the BDG consumed energy as $W_{bdg} = V_{bd}\ \rho_{bd}\ NCV_{bd}$. The electric work released to and consumed by all drives was measured by onboard grid analyzers, data being downloaded and processed after each route. These measurements were compared with the data obtained from the simulations described in Section 4.5.1 and reported in Table 7.

In the case of the Giudecca route, the final $SOC(T)$ of the LIB was 41% in good agreement with the results from eq. (5) of the model described in Section 4.5.1, confirming the estimated full emission abatement (100%) and energy expenditure saving (ca. 36%) in short routes. Fully recharging at $SOC(0) = 100\%$ from the dock recharging station took almost 6 h. In a drive test with modified EMS switch levels, also the whole Castello route (inside the historical city) was completed in full electric mode, i.e. with zero emission.

Longer routes, such as Murano and Islands of Table 1, were serviced in hybrid electric mode, with the BDG turned on ($S_{bdg} = 1$) when the SOC dropped to 35%. In particular, the final SOC of the LIB provided by the BMS after routing the Islands service was 23% (close to the values predicted by the simulations of the model of Section 4.5.1), with a fuel and emission abatement of 72% and energy expenditure saving of 20 %.

Fig. 10. A screenshot of the remote monitoring system, used for control and maintenance.

Table 8
Commissioning tests: peak power and work of the main drives in the five test reference routes. Prop = propulsion (propeller and steering), Comp = compactor, CrCoS = crane, cockpit and services.[1] The total drive peak power P_{dr} results from the simultaneous power demands from all power drives.[2] The total drive work W_{dr} is the sum of the work demands from all from all power drives along the whole route.

Routes	Peak power [kW]				Route work [kWh]			
	Prop	Comp	CrCoS	Tot Drive[1]	Prop	Comp	CrCoS	Tot Drive[2]
Cannaregio	48.0	47.5	12.2	53.5	32.7	8.2	1.1	42.0
Giudecca	49.2	24.9	12.2	55.2	42.9	6.1	1.7	50.7
Castello	48.1	18.3	12.2	54.1	54.5	5.0	1.2	60.7
Murano	49.3	27.1	12.2	55.4	79.0	7.8	1.7	88.5
Islands	49.9	22.5	12.2	56.0	90.0	6.5	1.8	98.3

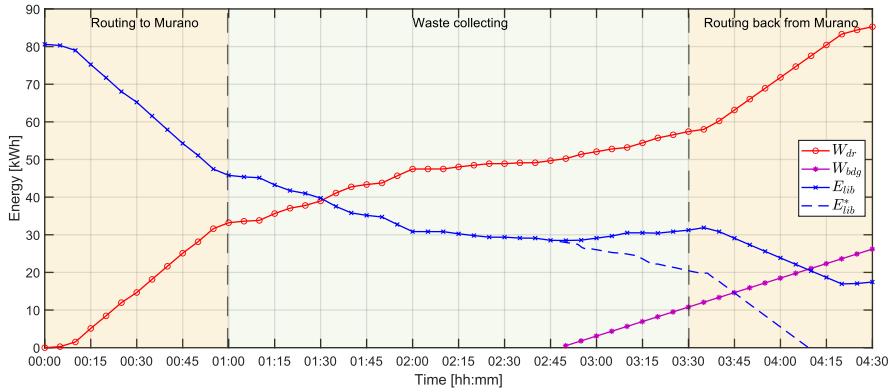

Fig. 11. Range-extender hybrid mode in the Murano route: the *SOC* dropped to 35% after 2:48 h of service, when the EMS started the BDG ($S_{bdg} = 1$) to slow down the battery energy decrease for extending its operation while delivering full power to the drives. W_{dr} = work demand from all drives; W_{bdg}= work delivered by the BDG and battery charger; E_{lib} = energy stored in the LIB; $E_{lib}{}^*$ = energy stored in the LIB if the BDG was not started.

Fully recharging at $SOC(0) = 100\%$ from the dock station took almost 7 h. The power/work consumed along the five reference routes are reported in Table 8. Fig. 11 illustrates the time profiles of the drive work demand W_{dr}, the battery stored energy E_{lib} and the work delivered by BDG W_{bdg} along the Murano route, that was driven in range-extender hybrid mode with the BDG switched on when the *SOC* dropped to 35% after 2:48 h of service, thus slowing the battery energy decrease while providing full power to the drives.

About 21,700 waste collection routes are driven yearly by Veritas boats, ca. 40% "short" and 60% "long", in 310 days of service. Considering the consumption data reported in this Section 5.2, over 610 tons of fuel and emissions and almost 170,000 € of energy cost could be saved if the whole fleet was converted to hybrid electric vessels like PHEB1. The adoption of a whole electric fleet is in the hands of VERITAS top management, who would take such a strategic decision not only on the basis of the results of this technological investigation and of the construction and service of a prototype here reported, but also on the ground of the expected time of transition to electric, of their investment plans and incentives and funding provided by local and national administrations which at present are not known. All these factors affect the future capital expenditure (CAPEX) for each vessel. However, such financial investigations are out of the scope of this paper, which aims to show the technical feasibility and advantages of vessel electrification, not only as regards emission abatement.

6. Conclusions

PHEB1 is a 12-m hybrid vessel capable of providing the same service as present ICE vessels at much lower environmental impact. It was put into regular service on different waste-collecting routes and it totalized over 500 operating hours by mid 2023. PHEB1 proved the advantages of the series hybrid powertrain for the waterborne service provided by Veritas waste collecting vessels, which can be considered a reference case for internal water and inland navigation. Its major advantage consists in strong emission abatements, but it can also provide notable benefits in terms of noise reduction, servicing work and operating cost reduction, as well as in maneuverability and pilot comfort. A further advantage consists in the strong reductions in total BDG running hours, with respect to an ICE boat, that translates into reduced maintenance costs and extended lifespan. Additionally, the electric propulsion and drives allow for an easier remote monitoring.

The series hybrid powertrain demonstrated to be compatible with the design constraints powering the onboard power drives which have been electrified. It demonstrated to be robust and flexible in the required service both in terms of power and work, operating in both all electric and hybrid range extender modes. It constitutes an interesting option for the next generation of waste-collecting boats that Veritas is going to introduce, in substitution of the present ICE fleet. Boats like PHEB1 promote the familiarization of the city authorities, economic operators, and dwellers with carbon-free electric water mobility, contributing to the acceptance of electric waterborne mobility in Venice, where most stakeholders have not yet undertaken firm steps toward decarbonized mobility. PHEB1 can demonstrate that these technologies are mature, accessible and friendly. In short, vessels like this are expected to increase the confidence toward a new decarbonized mobility paradigm in one of the most iconic cities in the world, visited every year by millions of tourists. While technology is progressing fast, urgent revisions and update of the maritime regulations are needed to promote and support the decarbonization of waterborne mobility. This is an international rather than Italian issue and it is desirable that the authorities like the European Commission and the European Parliament promote this evolution in the short term.

CRediT authorship contribution statement

Massimo Guarnieri: Writing – review & editing, Writing – original

draft, Validation, Supervision, Methodology, Investigation, Formal analysis, Conceptualization. **Angelo Bovo:** Validation, Supervision, Resources, Project administration, Funding acquisition, Data curation, Conceptualization. **Nicolò Zatta:** Writing – original draft, Formal analysis, Data curation. **Andrea Trovò:** Validation, Investigation, Data curation.

Declaration of competing interest

The authors declare that they have no known competing financial interests or personal relationships that could have appeared to influence the work reported in this paper.

Data availability

The authors do not have permission to share data.

Acknowledgments

AB acknowledges financial support from the Italian Ministry for Environment and Land and Sea Protection and the Venetian Municipality. MG, AT and NZ acknowledge support from the Interdepartmental Centre Giorgio Levi Cases for Energy Economics and Technology, of the University of Padua, Italy, within the project GUARRICERCALASCITOLEVI 20-01.

References

[1] Nia P, Wang X, Li H. A review on regulations, current status, effects and reduction strategies of emissions for marine diesel engines. Fuel 2020;279:118477. https://doi.org/10.1016/j.fuel.2020.118477.
[2] Unknown author, First fuel cell passenger ship unveiled in Hamburg. Fuel Cell Bull 2008;10:4–5. https://doi.org/10.1016/S1464-2859(08)70372-9.
[3] Unknown author, U212/U214 submarines, naval technology, 2020 [Online], http://www.naval-technology.com/projects/type_212/. [Accessed 6 January 2024].
[4] Köhlmoos A, Bertram V, Hoffmeister H, Hansen H, Moltschaniwskyj A. Design by best engineering principles for the solar catamaran Tûranor planetsolar. 4th high performance yacht design conference 2012. HPYD; 2012. p. 163–71.
[5] Shahan C. World's first all-electric battery-powered ferry. Clean Technica; June 13, 2015. https://cleantechnica.com/2015/06/13/worlds-first-electric-battery-powered-ferry/. 06/01/2024.
[6] Allied Market Research. Electric boat market. https://www.alliedmarketresearch.com/electric-boat-market-A08766. [Accessed 6 January 2024].
[7] Markets and markets, electric ship market. https://www.marketsandmarkets.com/Market-Reports/electric-ships-market-167955093.html. [Accessed 6 January 2024].
[8] Hansen J, Wendt F. History and state of the art in commercial electric ship propulsion, integrated power systems, and future trends. Proc IEEE 2015;103(212):2229–42.
[9] Doerry N, Amy J, Krolick C. History and the status of electric ship propulsion, integrated power systems, and future trends in the U.S. Navy. Proc IEEE 2015;103(212):2243–51.
[10] Skjong E, Rødskar E, Molinas M, Johansen TA, Cunningham J. The marine vessel's electrical power system: from its birth to present day. Proc IEEE 2015;103(12):2410–24. https://doi.org/10.1109/JPROC.2015.2496722.
[11] Paul D. A history of electric ship propulsion systems. IEEE Ind Appl Mag 2020;26(6):9–19. https://doi.org/10.1109/MIAS.2020.3014837.
[12] McCoy TJ. Electric ships past, present, and future. IEEE Electrif. Mag. 2015;3(2):4–11. https://doi.org/10.1109/MELE.2015.2414291.
[13] Skjong E, Volden R, Rodskar E, Molinas M, Johansen TA, Cunningham J. Past, present, and future challenges of the marine vessel's electrical power system. IEEE Trans. Transp. Electrification 2016;2(4):522–37. https://doi.org/10.1109/TTE.2016.2552720.
[14] Kondo A, Hirose Y. Effects of introduction of a water-bus system and transport policies on road traffic and the environment in urban areas. Proc. Int. Conf. Urban Transport and Environment 21st Century, Lisbon, Portugal 1998:115–26. https://doi.org/10.2495/UT980121.
[15] Spagnolo G, Papalilo D, Martocchia A. Eco friendly electric propulsion boat. Proc. 10th int. Conf. Environment and electrical engineering (EEEIC.EU 2011). 2011. https://doi.org/10.1109/EEEIC.2011.5874699. Rome.
[16] Stanciu V, Chefneux M, Anghelita P, Varaticeanu B. Hybrid propulsion conceptual model for watercraft: eco-boat. Electrotechnica Electrinica Automatica 2012;60(4):78–88.
[17] Pecorari E, Menegaldo M, Innocente E, Ferrari A, Giuponi G, Cuzzolin G, Rampazzo G. On which grounds a decision is taken in waterborne transport technology to reduce air pollution? Atmos Pollut Res 2020;11(12):2088–99. https://doi.org/10.1016/j.apr.2020.07.018.
[18] Guarnieri M, Bovo A, Giovannelli A, Mattavelli P. A real multitechnology microgrid in Venice: a design review. IEEE Ind. Electron. Mag. 2018;12(3):19–31. https://doi.org/10.1109/MIE.2018.2855735.
[19] Chalfant J. Early-stage design for electric ship. Proc IEEE 2015;103(12):2252–66. https://doi.org/10.1109/JPROC.2015.2459672.
[20] Mcnabb J, Robertson NA, Steffens M, Sudol A, Mavris D, Chalfant J. Exploring the design space of an electric ship using a probabilistic technology evaluation methodology. Proc. 2019 IEEE Electric Ship Technologies Symp, ESTS 2019; 8847846:181–8. https://doi.org/10.1109/ESTS.2019.8847846. 2019, Washington DC (US).
[21] McCoy TJ, Amy JV. The state-of-the-art of integrated electric power and propulsion systems and technologies on ships. Proc. 2009 IEEE electric ship technologies symp., ESTS 2009. Baltimore: US-MD); 2009. p. 340–4. https://doi.org/10.1109/ESTS.2009.4906534.
[22] McCoy TJ. Integrated power systems: an outline of requirements and functionalities for ships. Proc IEEE 2015;103(12):2276–84. https://doi.org/10.1109/JPROC.2015.2480597.
[23] Zahedi B, Norum LE, Ludvigsen KB. Optimized efficiency of all-electric ships by dc hybrid power systems. J Power Sources 2014;255:341–54. https://doi.org/10.1016/j.jpowsour.2014.01.031.
[24] Kim S-Y, Choe S, Ko S, Sul SK. A naval integrated power system with a battery energy storage system: fuel efficiency, reliability, and quality of power. IEEE Electrific. Mag. 2015;3(2):22–33. https://doi.org/10.1109/MELE.2015.2413435.
[25] Sulligoi G, Vicenzutti A, Menis R. All-electric ship design: from electrical propulsion to integrated electrical and electronic power systems. IEEE Trans. Transp. Electrification 2016;2(4):507–21. https://doi.org/10.1109/TTE.2016.2598078.
[26] Thongam JS, Tarbouchi M, Okou AF, Bouchard D, Beguenane R. All-electric ships - a review of the present state of the art. Proc. 8th International Conference and Exhibition on Ecological Vehicles and Renewable Energies, EVER 2013, Montecarlo (Monaco) 2013;4:6521626. https://doi.org/10.1109/EVER.2013.6521626.
[27] Khersonsky Yuri. Advancing new technologies in electrical ships: IEEE standards are the risk mitigation tool, IEEE electrif. Mag. 2015;3(2):34–9. https://doi.org/10.1109/MELE.2015.2414031.
[28] Kim K, Park K, Ahn J, Roh G, Chun K. A study on applicability of battery energy storage system (BESS) for electric propulsion ships. Proc. 2016 IEEE transportation electrification conference and expo, asia - pacific (ITEC), busan (korea). 2016. p. 203–7. https://doi.org/10.1109/ITEC-AP.2016.7512948.
[29] Malla U. Design and sizing of battery system for electric yacht and ferry. Int J Interact Des Manuf 2020;14(1):137–42.
[30] Kim K, Park K, Lee J, Chun K, Lee S-H. Analysis of battery/generator hybrid container ship for CO2 reduction. IEEE Access 2018;6(14):537–43.
[31] Zahedi B, Norum LE. Modeling and simulation of all-electric ships with low-voltage DC hybrid power systems. IEEE Trans Power Electron 2013;28(10):4525–37. https://doi.org/10.1109/TPEL.2012.2231884.
[32] Kanellos FD, Tsekouras GJ, Hatziargyriou ND. Optimal demand-side management and power generation scheduling in an all-electric ship. IEEE Trans Sustain Energy 2014;5(4):1166–75. https://doi.org/10.1109/TSTE.2014.2336973.
[33] Kanellos FD. Optimal power management with GHG emissions limitation in all-electric ship power systems comprising energy storage systems. IEEE Trans Power Syst 2014;29(1):330–9. https://doi.org/10.1109/TPWRS.2013.2280064.
[34] Vu TV, Gonsoulin D, Perkins D, Diaz F, Vahedi H, Edrington CS. Predictive energy management for MVDC all-electric ships. Proc. 2017 IEEE electric ship technologies symp, ESTS 2017. Arlington (US-VA); 2014. p. 327–31. https://doi.org/10.1109/ESTS.2017.8069302.
[35] Cupelli M, Ponci F, Sulligoi G, Vicenzutti A, Edrington CS, El-Mezyani T, T, Monti A. Power flow control and network stability in an all-electric ship. Proc IEEE 2015;103(12):2355–80. https://doi.org/10.1109/JPROC.2015.2496789.
[36] Hebner RE. Electric ship power system - research at the university of Texas at austin. Proc. 2005 IEEE Electric Ship Technologies Symp., ESTS 2005 25-27 July 2005:34–8. https://doi.org/10.1109/ESTS.2005.1524649. Philadelphia (US-PA).
[37] Geertsma RD, Negenborn RR, Visser K, Hopman JJ. Design and control of hybrid power and propulsion systems for smart ships: a review of developments. Appl Energy 2017;194:30–54. https://doi.org/10.1016/j.apenergy.2017.02.060.
[38] Barros J, Diego RI. A review of measurement and analysis of electric power quality on shipboard power system networks. Renew. Sust. Energ. Rev. 2016;62:665–72. https://doi.org/10.1016/j.rser.2016.05.043.
[39] Nuchturee C, Li T, Xia H. Energy efficiency of integrated electric propulsion for ships – a review. Renew. Sust. Energ. Rev. 2020;134:110145. https://doi.org/10.1016/j.rser.2020.110145.
[40] Balestra L, Schjølberg I. Modelling and simulation of a zero-emission hybrid power plant for a domestic ferry. Int J Hydrogen Energy 2021;46:10924–38. https://doi.org/10.1016/j.ijhydene.2020.12.187.
[41] Yuan Y, Wang J, Yan X, Shen B, Long T. A review of multi-energy hybrid power system for ships. Renew. Sust. Energ. Rev. 2020;132:110081. https://doi.org/10.1016/j.rser.2020.110081.
[42] Perčić M, Vladimir N, Fan A. Life-cycle cost assessment of alternative marine fuels to reduce the carbon footprint in short-sea shipping: a case study of Croatia. Appl Energy 2020;279:115848. https://doi.org/10.1016/j.apenergy.2020.115848.
[43] Kim S-Y, Yoon Y-D, Sul S-K. Suppression of the thrust loss for the maximum thrust operation in the electric propulsion ship. Proc. 2007 IEEE electric ship technologies symp, ESTS 2007, arlington (US-va). 21-23 May 2007. p. 72–6. https://doi.org/10.1109/ESTS.2007.372066.

[44] Qazi S, Venugopal P, Rietveld G, Soeiro TB, hipurkar SU, Grasman A, Watson AJ, Wheeler P. Powering Maritime: challenges and prospects in ship electrification. IEEE Electrif. Mag. 2023;11(2):74–87. https://doi.org/10.1109/MELE.2023.3264926.
[45] Postiglione CS, Collier DAF, Dupczak BS, Heldwein ML, Perin AJ. Propulsion system for an all electric passenger boat employing permanent magnet synchronous motors and modern power electronics, Electrical Systems for Aircraft, Railway and Ship Propulsion. ESARS 2012:6387441. https://doi.org/10.1109/ESARS.2012.6387441.
[46] Guarnieri M, Morandin M, Campostrini P, Ferrari A, Bolognani S. Electrifying water buses: a case study on diesel-to-electric conversion in Venice. IEEE Ind Appl Mag 2018;24(1):71–83. https://doi.org/10.1109/MIAS.2017.2739998.
[47] Balsamo F, Capasso C, Lauria D, Veneri O. Optimal design and energy management of hybrid storage systems for marine propulsion applications. Appl Energy 2020;278:115629. https://doi.org/10.1016/j.apenergy.2020.115629.
[48] Miretti F, Misul D, Gennaro G, Ferrari A. Hybridizing waterborne transport: modeling and simulation of low-emissions hybrid waterbuses for the city of Venice. Energy 2022;244:123183. https://doi.org/10.1016/j.energy.2022.123183. Part B.
[49] Han J, Charpentier J-F, Tang T. An energy management system of a fuel cell/battery hybrid boat. Energies 2014;7:2799–820. https://doi.org/10.3390/en7052799.
[50] Su C-L, Guerrero JM, Chen S-H. Happiness is a hybrid - electric: a diesel-burning boat finds new life with a direct-current microgrid. IEEE Spectrum 2019;56(8):42–7. https://doi.org/10.1109/MSPEC.2019.8784122.
[51] Letafat A, Rafiei M, Ardeshiri M, Sheikh M, Banaei M, Boudjadar J, Khooban M-H. An efficient and cost-effective power scheduling in zero-emission ferry ships. Complexity 2020. https://doi.org/10.1155/2020/6487873.
[52] E. Mattarelli, C.A. Rinaldini, T. Savioli, A. Warey et al., An innovative hybrid powertrain for small and medium boats, SAE Technical Paper, 2018 SAE World Congress Experience, Detroit (US-MI), 134884. DOI: 10.4271/2018-01-0373.
[53] De Putter T. Cobalt means conflict – Congolese Cobalt, a critical element in lithium-ion batteries. Bulletin des Séances - Mededelingen der Zittingen 2021;65(1):97–110. https://doi.org/10.5281/zenodo.4604403.
[54] Kaniki AK, Tumba K. Management of mineral processing tailings and metallurgical slags of the Congolese copperbelt: environmental stakes and perspectives. J Clean Prod 2019;210:1406–13. https://doi.org/10.1016/j.jclepro.2018.11.131.
[55] IEA - International Energy Agency. The role of critical minerals in clean energy transitions - world energy outlook special report. Revised version March 2022, https://www.iea.org/reports/the-role-of-critical-minerals-in-clean-energy-transitions. [Accessed 12 September 2022].
[56] Whittingham MS. Lithium batteries and cathode materials. Chem. Rev. 2004;104(10):4271–301. https://doi.org/10.1021/cr020731c.
[57] Swain B. Recovery and recycling of lithium: a review. Sep Purif Technol 2017;172:388–403. https://doi.org/10.1016/j.seppur.2016.08.031.
[58] Zubi G, Dufo-López R, Carvalho M, Pasaoglu G. The lithium-ion battery: state of the art and future perspectives. Renew. Sust. Energ. Rev. 2018;89:292–308. https://doi.org/10.1016/j.rser.2018.03.002.
[59] Dubarry M, Liaw B-L. Identify capacity fading mechanism in a commercial LiFePO4 cell. J Power Sources 2009;194:541–9. https://doi.org/10.1016/j.jpowsour.2009.05.036.
[60] Mousavi G SM, Nikdel M. Various battery models for various simulation studies and applications. Renew. Sust. Energ. Rev. 2014;32:477–85. https://doi.org/10.1016/j.rser.2014.01.048.
[61] Tremblay O, Dessaint L-A. Experimental validation of a battery dynamic model for EV applications. World Electr. Veh. J. 2009;3(2):289–98. https://doi.org/10.3390/wevj302028.
[62] Mahdi H, Hoff B, Østrem T. A review of power converters for ships electrification. IEEE Trans Power Electron 2023;38(4):4680–97. https://doi.org/10.1109/TPEL.2022.3227398.
[63] Ritari A, Huotari J, Halme J, Tammi K. Hybrid electric topology for short sea ships with high auxiliary power availability requirement. Energy 2020;190:116359. https://doi.org/10.1016/j.energy.2019.116359.
[64] Hannan MA, Lipu MSH, Hussain A, Mohamed A. A review of lithium-ion battery state of charge estimation and management system in electric vehicle applications: challenges and recommendations. Renew. Sust. Energ. Rev. 2017;78:834–54. https://doi.org/10.1016/j.rser.2017.05.001.
[65] Wang X, He H, Sun F, Sun X, Tang H. Comparative study on different energy management strategies for plug-in hybrid electric vehicles. Energies 2013;6:5656–75. https://doi.org/10.3390/en6115656.
[66] Bassam AM, Phillips AB, Turnock SR, Wilson PA. An improved energy management strategy for a hybrid fuel cell/battery passenger vessel. Int. J. Hydrog. Energy 2016;41(47):22453–64. https://doi.org/10.1016/j.ijhydene.2016.08.049.
[67] Sulaimana N, Hannanb MA, Mohamedc A, Kerb PJ, Majlana EH, Wan Dauda WR. Optimization of energy management system for fuel-cell hybrid electric vehicles: issues and recommendations. Appl Energy 2018;228:2061–79. https://doi.org/10.1016/j.apenergy.2018.07.087.
[68] Gao D, Jin Z, Lu Q. Energy management strategy based on fuzzy logic for a fuel cell hybrid bus. J Power Sources 2008;185:311–7. https://doi.org/10.1016/j.jpowsour.2008.06.083.
[69] Moura SJ, Callaway DS, Fathy HK, Stein JL. Tradeoffs between battery energy capacity and stochastic optimal power management in plug-in hybrid electric vehicles. J Power Sources 2010;195:2979–88. https://doi.org/10.1016/j.jpowsour.2009.11.026.
[70] Paganelli G, Delprat S, Guerra T-M, Rimaux J, Santin J-J. Equivalent consumption minimization strategy for parallel hybrid powertrains. IEEE 55th Vehicular technology conference, VTC Spring 2002;4:2076–81. https://doi.org/10.1109/VTC.2002.1002989.
[71] Bassam AM, Phillips AB, Turnock SR, Wilson PA. Development of a multi-scheme energy management strategy for a hybrid fuel cell driven passenger ship. Int. J. Hydrog. Energy 2017;42:623–35. https://doi.org/10.1016/j.ijhydene.2016.08.209.
[72] Bruzzese C, Tessarolo A, Mazzuca T, Scala G. A closer look to conventional hydraulic ship actuator systems and the convenience of shifting to (possibly) all-electric drives. IEEE electric ship technologies symposium (ESTS). 2013. p. 220–7. https://doi.org/10.1109/ESTS.2013.6523738. Arlington, VA, USA.
[73] Romare M, Dahllöf L. The life cycle energy consumption and greenhouse gas emissions from lithium-ion batteries. IVL Swedish Environmental Research Institute; 2017. Report C243, https://www.energimyndigheten.se/globalassets/forskning–innovation/transporter/c243-the-life-cycle-energy-consumption-and-co2-emissions-from-lithium-ion-batteries-.pdf. [Accessed 6 January 2024].